Applied Catalysis B: Environmental 165 (2015) 185–191

Contents lists available at ScienceDirect

Applied Catalysis B: Environmental

journal homepage: www.elsevier.com/locate/apcatb

Electrochemical growth of platinum nanostructures for enhanced ethanol oxidation

L.Q. Wang[a,b], M. Bevilacqua[a], J. Filippi[a], P. Fornasiero[b], M. Innocenti[a,c], A. Lavacchi[a,*], A. Marchionni[a], H.A. Miller[a], F. Vizza[a,**]

[a] ICCOM-CNR, Via Madonna del Piano 10, 50019 Sesto Fiorentino (FI), Italy
[b] Department of Chemical and Pharmaceutical Sciences, University of Trieste, Via L. Giorgieri 1, 34127 Trieste, Italy
[c] Dipartimento di Chimica, Università di Firenze, Via della Lastruccia 3, 50019 Sesto Fiorentino (FI), Italy

ARTICLE INFO

Article history:
Received 18 June 2014
Received in revised form
24 September 2014
Accepted 3 October 2014
Available online 14 October 2014

Keywords:
Platinum nanostructures
Ethanol oxidation
Electrocatalysis
Biomass
In situ spectroelectrochemistry

ABSTRACT

The catalytic activation of polycrystalline platinum toward ethanol electro-oxidation in alkaline environment has been obtained by a square wave potential treatment.

A detailed analysis that explores the effect of the period of the square wave on the evolution of the catalytic properties of the Pt surface is reported. The catalytic behavior of the treated and untreated surfaces has been interpreted both in terms of real surface area and surface structure evolution.

The most active surface has been produced with a treating period time of 120 min. Interestingly the maximum stability has been obtained with the sample produced with square wave potential with a period of 360 min with slightly lower initial performance.

We have also found that the treated samples limit C—C cleavage, as compared to bare Pt, offering an effective strategy to minimize the formation of CO. Via in situ FTIR we have demonstrated that the major oxidation product is acetate. These findings are especially important in view of the application of Pt as a catalyst in alkaline direct ethanol fuel cells.

1. Introduction

To date platinum is still the most commonly exploited material in electrocatalysis. This is because of its good catalytic activity in a variety of energy related electrochemical reactions together with outstanding corrosion resistance in both alkaline and acidic environments [1–4]. Indeed polymer electrolyte membrane fuel cell (PEMFCs) technology, often considered as the ultimate solution to automotive powering, heavily relies on platinum for catalyzing both hydrogen oxidation and oxygen reduction [5].

Platinum has also been proved to be effective for the catalysis of electrochemical oxidation of a variety of small organic molecules (SOMs) [6–9]. For this reason it has been applied as active phase at the anode and cathode of alcohol fed fuel cells with the main target of building a new generation of power sources for portable applications. Among these alcohols, methanol has certainly been the most widely explored [8,10,11]. Despite decades of research methanol fuel cells are not yet a well-established commercial technology, mainly due to the instability of these devices and the relatively poor performance as compared to PEMFCs. More recently ethanol has entered onto the scene. It has the advantage over methanol of being easily produced with well-established technology from biomasses [12]. Furthermore ethanol is less volatile and far less toxic than methanol, also being easy to store, handle and transport. For all of these promising aspects, ethanol electro-oxidation in fuel cells is an issue of outstanding importance, being at the same time an extraordinarily challenging research topic [7,9,12,13]. Platinum and PtRu have been shown to be effective catalysts for alcohol electrooxidation [7,9,14,15]. Recently PtSn alloys have been proved to be even more performing exhibiting good activity in complete direct ethanol fuel cells tests [16–19]. Nevertheless the use of platinum raises two main concerns related to its practical exploitation: (i) the need for high metal loadings [8,20] and (ii) CO poisoning [21,22]. The need for high Pt loadings poses severe limitations, as the scarcity of platinum resources limits its use to applications where it is absolutely unavoidable. Recently the European Union has classified platinum among the so-called "critical raw materials", stressing both on its technological relevance and rarity [23,24]. The US Department of Energy periodically publishes reports on future technology targets [25]. Lately a platinum

* Corresponding author. Tel.: +61 390555225250; fax: +39 0555225203.
** Corresponding author. Tel.: +61 390555225286; fax: +39 0555225203.
E-mail addresses: alessandro.lavacchi@iccom.cnr.it (A. Lavacchi), francesco.vizza@iccom.cnr.it (F. Vizza).

http://dx.doi.org/10.1016/j.apcatb.2014.10.009
0926-3373/

content of 0.125 mg cm^{-2} for automotive PEMFCs has been fixed as an objective to be achieved by 2017. This figure is believed to be reasonably good to guarantee the sustainability of platinum supply in the case of a full technological and commercial exploitation. Remarkably for PEMFCs no conventional supported high surface area platinum material has yet met such a target [26]. At present only nano structured thin films (NSTF) have been shown to be active enough to meet the requirements. CO poisoning is critical for PEMFCs and even more for direct alcohol fuel cells (DAFCs). It is well known that the electro-oxidation of ethanol may result in the production of CH_3CHO (unstable in alkali), CH_3COOH (CH_3COO^- in alkali) and CO_2 (CO_3^{2-} in alkali). CO, as an intermediate product may occur in case of C—C cleavage. The addition of ruthenium to platinum promotes CO oxidation and elimination, but CO poisoning is still an issue [27–33].

In order to overcome the problem of CO production it has been demonstrated, at least with Pd catalysts [34], that it is convenient to operate in alkaline conditions, where the C—C cleavage of ethanol has been shown to be hampered resulting in negligible production of C_1 fragments. While this could appear a limitation, in principle, as only four electrons are transferred, it is worth mentioning that to date the most energy efficient direct ethanol fuel cells are those operating in alkaline conditions resulting in the production of acetate. This is because no catalyst that produces effective C—C cleavage is actually known. Indeed the complete oxidation of ethanol to CO_2 or carbonate has very sluggish kinetics [35–39]. These kinetic drawbacks lower fuel cell performance despite the fact of having, in principle up to 12 exchanged electrons.

In the present work we introduce a new approach to the activation of platinum surfaces for application in ethanol electro-oxidation in alkaline environment. Inspiration was taken from a previous paper reporting an analogous procedure for Pd. In that work a square wave potential with fixed frequency was chosen to activate the Pd surface. The procedure was successful in generating nanostructured highly active Pd electrocatalysts [40,41]. Here we show that Pt requires different treatment conditions as compared to Pd. Particularly the dependence on the frequency of the square wave treatment in ethanol electro-oxidation activity in alkaline environment is reported here for the first time.

2. Materials and methods

In all the electrochemical experiments, a polycrystalline Pt disk with a geometric surface area of 0.1963 cm^2 was used as working electrode. The counter electrode was a platinum wire (0.5 mm diameter) while the reference electrode was a KCl saturated Ag/AgCl electrode. All potentials are reported against the reference hydrogen electrode (RHE). RHE potentials were calculated accounting for the hydrogen ion activity in the investigated electrolyte.

The treatment of the polycrystalline Pt foil was performed with a fixed duration of 360 min. through a repetitive square wave potential bounded between 4.55 V and −1.95 V (RHE) in 2 M KOH electrolyte. Wave periods of 6 min (60 full waves), 60 min (6 full waves), 120 min (3 full waves), 180 min (2 full waves), 360 min (1 full wave) were selected for the synthesis of the samples.

Electrochemical measurements were performed with a PARSTAT 2273 potentiostat/galvanostat (Princeton Applied Research, USA) in a three-electrode cell arrangement at room temperature. All the solutions were purged with N_2 for 15 min before any electrochemical experiment. Before each square wave treatment the Pt electrode surface was mechanically polished with polycrystalline diamond suspension down to 1 μm. Electrodes were subsequently washed in a FALC ultra-sonic bath for 15 min. At the end of each square wave potential treatment, the electrode was cleaned with doubly distilled-deionized water.

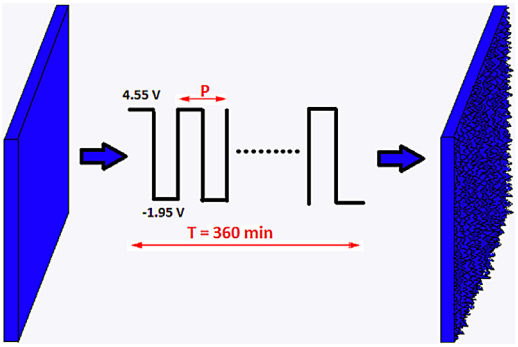

Fig. 1. Schematics of the square wave treatment. Roughness is enhanced by the application of the square wave potential. All the treatments applied had a duration of 360 min. The period (*P*) of the square wave was varied between 6 min (60 full wave) and 360 min (1 full wave).

The electrochemically active surface area (EASA) of this electrode was determined by integration of the charge in the hydrogen region of the cyclic voltammograms (CVs) between 0.05 and 0.4 V in 0.5 M H_2SO_4 solution [42]. The activity for ethanol oxidation was investigated in 2 M ethanol + 2 M KOH by cyclic voltammetry between 0.05 and 0.70 V. All of the CVs were repeated until curves were obtained with high stabilization. The reported CVs were acquired at a scan rate of 50 mV/s. Chronoamperometry was performed at 0.5 V vs. RHE for 3600 s.

Electrochemical in situ FTIR reflection spectroscopy was performed on a Nicolet 6700 spectrometer equipped with a DTGS detector. Prior to the acquisition of the reference spectrum the electrode has been cleaned in 0.1 M $HClO_4$ in the 0.0–1.0 V RHE potential window. The electrode has been then introduced in the FTIR cell imposing a 0.0 V RHE potential. The reference spectrum has been collected after 2 min from the electrode immersion for both the treated and the untreated Pt. Spectra have been acquired at the same potential values and with the same acquisition time for both samples to allow a direct comparison.

The spectro-electrochemical cell was designed to have the Pt electrode supported by a CaF_2 window. Such configuration allows only a thin film of electrolyte (10 μm range) to be in the gap between the electrode and the window. Each spectrum was determined averaging 128 interferograms acquired with a resolution of 4 cm^{-1}. The reference spectrum (R_{ref}) was collected at 0 V vs. RHE. Potential steps were set to 0.1 V until 1.2 V has been reached. Spectra were normalized according to Eq. (1) [43].

$$\frac{\Delta R}{R} = \frac{R_s - R_{ref}}{R_{ref}} \quad (1)$$

Under such a representation scheme, negative and positive bands correspond to produced and consumed species respectively.

Electron microscopy was performed with a field emission scanning electron microscopes Zeiss Gemini 1530, capable of a spatial resolution 2.1 nm at 1.0 kV.

3. Results and discussion

The platinum activation with square wave potential is performed according to the treatment schematized in Fig. 1.

Inspiration was taken from our previous studies on the application of a square wave potential to activate the surface of Pd leading to very active nanostructured electrocatalysts [40,41]. Nevertheless, the nature of Pt oxidation is different from that of Pd, so major adaptation has been required to accomplish the task of enhancing electrocatalytic activity for Pt. Indeed it has been previously

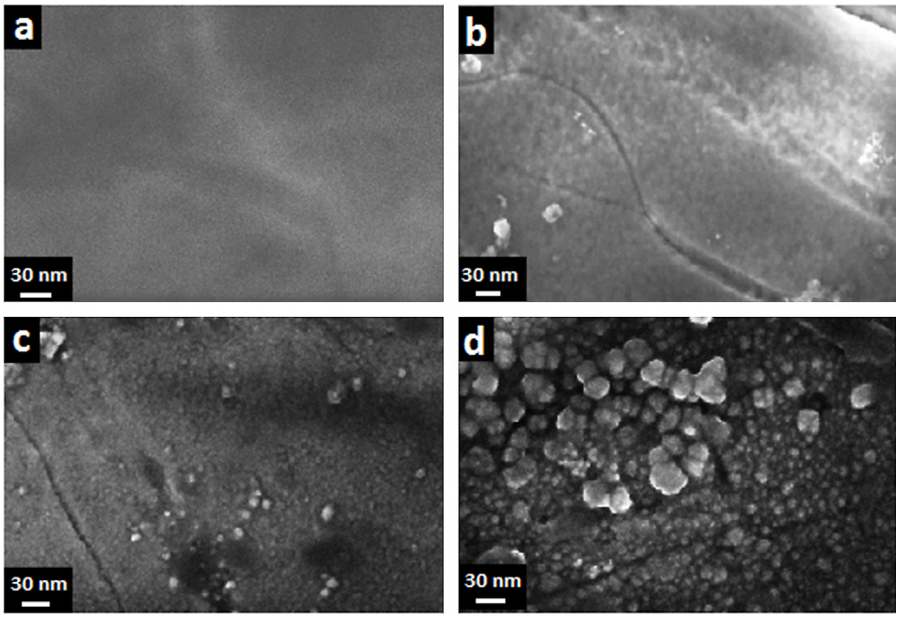

Fig. 2. Microscopy reveals morphology changes induced by the treatment. FESEM images of Pt surfaces after electrochemical treatment with different treated cycle time: (a) pristine Pt surface, after square wave treatment with period of (a) 6 min, (b) 120 min, (c) 360 min.

reported that a prolonged oxidation of a platinum surface produces the growth of an incoherent and rough oxides with island structures. The formation of such structures requires the overcoming of an induction time as their growth has been reported to be strongly time-dependent [44]. We hypothesized that such roughening could be used for increasing the surface area of platinum eventually also resulting in modification of the surface structure. With this in mind we propose an approach based on the application of a square wave potential to platinum, to produce nanostructured metallic platinum surfaces with enhanced catalytic properties toward ethanol oxidation in alkaline environment. The dependency on the frequency (data in the paper are reported against the period for simplifying the numbers) of square wave and of both morphology and catalytic activity have also been explored.

Surface evolution as a result of the application of various treatments was investigated by field emission scanning electron microscopy. A set of three samples obtained with 6, 120 and 360 min periods was selected for such a characterization. Fig. 2 clearly shows that for a period of 6 min surface nano-structuring occurs.

The roughness evolution results as a consequence of the morphology evolution occurring during platinum oxidation. It has been shown that when platinum oxidation is performed concurrently with oxygen evolution roughening occurs as reported by Brian E. Conway [44]. Interestingly, such roughening requires first overcoming an induction time, usually of the order of minutes [44]. For times shorter than the induction time the formation of the oxide scale is coherent with the morphology of the substrate, producing no significant alteration of the roughness. Oxidation times longer than a few minutes produce the formation of columnar islands. The formation of columnar structures is revealed by a net increase in the oxidation current. Furthermore roughening may also be ascribed to platinum dissolution and re-deposition. Platinum dissolution may occur at high potentials [45]. Consistently re-deposition of dissolved platinum could be considered responsible for the formation of the largest nanostructures shown on Fig. 2d. This also indicates that the metal dissolved can be recovered from the solution by subsequent electrodeposition.

To give a quantitative assessment of the extent of roughening, CVs in 0.5 M H_2SO_4 was recorded (Fig. 3). The EASA has been determined [42] from the hydrogen adsorption and desorption charge after stabilization (10 cycles). Table 1 shows that even the samples treated with the shorter wave period (6 min) the EASA is enhanced by a factor 2.45. A fourfold enhancement was obtained for the 360 min wave period.

A more detailed analysis of the CVs in the hydrogen adsorption/desorption region (<0.35 V) reveals changes in the distribution of the crystal terminations (Fig. 3a). The two peaks, observed at

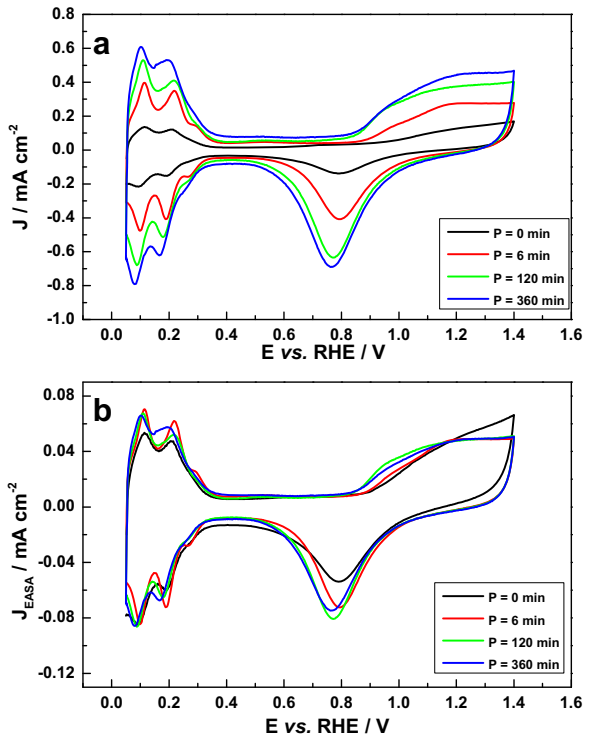

Fig. 3. Cyclic voltammetry explains the surface modifications induced the treatment. CVs in 0.5 M H_2SO_4 at a scan rate of 50 mV/s normalized by geometric area (a) and normalized by the EASA (b).

Table 1
Active surface area of electrochemical treated Pt.

Period (min)	Active surface area (cm^2)
0	1.806
6	4.433
120	6.177
360	7.246

the anodic scan of 0.11 V and 0.22 V, in UPD-H (under deposition hydrogen) of the untreated sample can be attributed to H desorption on (1 1 0) and (1 0 0) sites respectively [46–48]. No clear H-desorption peak but a weak shoulder at 0.29 V possibly corresponding to the large (1 0 0) domains can be observed [49,50]. The hydrogen adsorption peaks position and current density change as a result of the treatment indicating the changing of the distribution of facets [51]. Surface structure evolution is also supported by the analysis of the CVs in the Pt oxidation region (>0.8 V). Pt oxidation is known to proceed via a two-step mechanism [44] according to Eqs. (2) and (3).

$$Pt + H_2O \rightarrow Pt(OH)_{ads} + H^+ + e^- \quad (2)$$

$$Pt(OH)_{ads} \rightarrow PtO + H^+ + e^- \quad (3)$$

Eq. (2) is referred to the formation of a surface hydroxide while Eq. (3) represents the formation of the surface Pt oxide. Eqs. (2) and (3) together are the electrochemical reactions that account for the anodic current density in the Pt oxidation region of the CV.

It has been shown that an increase in the EASA normalized current density for Pt oxidation at potential lower than 1.0 V is an indication of the presence of a larger density of poorly coordinated platinum atoms. It is indeed known that platinum sites with low coordination number show much larger tendency to oxidation as compared to high coordination sites. The larger stability of such oxide results in the cathodic shift of the peak attributed to the reduction of the oxide as well [44]. The high density of low coordination surface atoms, while detrimental to oxygen reduction reaction [52], has been proved to promote the electro-catalytic oxidation of small organic molecules [6,53]. In Fig. 3b it is evident that amongst all the investigated samples the 120 min shows the largest EASA normalized current density under 1.0 V. Notably this is also the sample showing the largest ethanol oxidation activity as will be shown later. According to this we can conclude that the sample obtained at 120 min is the one showing the larger density of poorly coordinated Pt surface atoms [53]. For square wave period larger than 120 min such a density slightly diminishes. This could be explained considering that longer time produces a thicker oxide scale whose reduction results in the formation of larger nanostructures. Furthermore, as observed by FESEM investigation, re-deposition of dissolved platinum cannot be excluded leading to a completely different mechanism, which in principle could favor formation of more thermodynamically stable surfaces.

Electrocatalytic activity was assessed toward ethanol electrooxidation in alkaline media. It has been reported by Zhao [54] and Shen [55] that higher ethanol and KOH concentration are required to get higher adsorption of ethoxy and hydroxyl yielding an increase in an oxidation current of EOR. In addition, a 2 M ethanol 2 M KOH solution electrolyte has been selected as it has been shown to be employed in the most performing direct alcohols fuel cells [12,41,56]. The first half voltammetric cycles sweep between 0.05 V and 0.70 V and is shown in Fig. 4a. The positive potential limit was chosen to avoid the onset of the surface oxidation. Such an oxidation could indeed result in changes of the surface structure also producing reduction of the surface area through the so-called electrochemical annealing [57]. Fig. 4a shows that all the treated Pt electrodes deliver better performance as compared to the untreated one. As previously anticipated the best electro-catalytic activity is

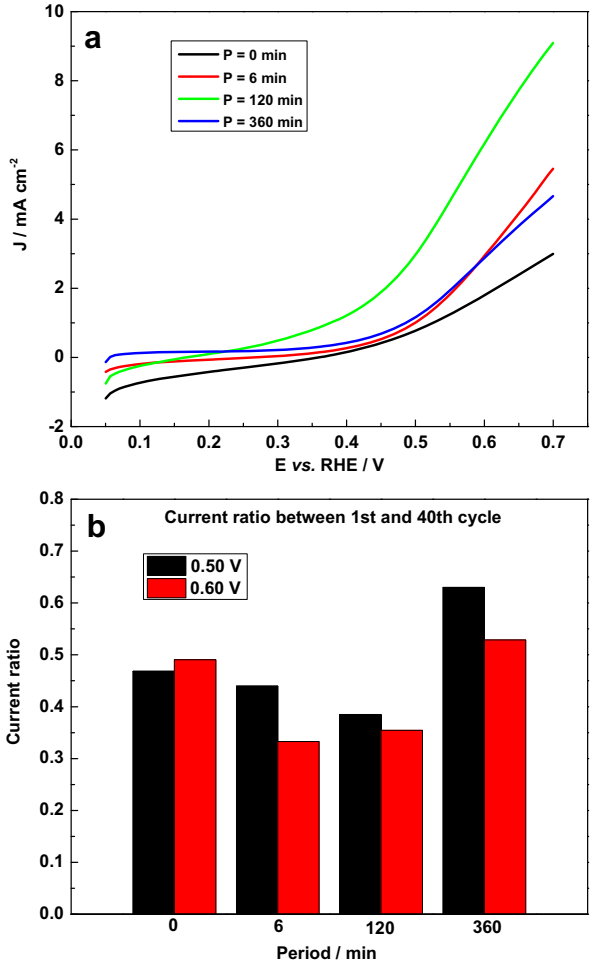

Fig. 4. Electrocatalytic performance improves as a result of the surface modifications induced by the treatment. First positive sweep of the CVs in 2 M ethanol 2 M KOH electrolyte (a) and current density ratio between the first and the fortieth cycle at 0.50 V and 0.60 V (b). The current is normalized by geometric area.

obtained with the 120 min period sample. In fact, a current density of 6.05 mA/cm^2 at 0.6 V was recorded by CV for the 120 min samples while the untreated sample only delivered 1.75 mA/cm^2 (Table 2). Different voltammetric profiles can be found for Pt with different treated period. In addition to the differences in the general shape of the voltammetric curves, a structural effect can also be observed in the onset potentials of the reaction and in the total currents. All the treated Pt samples show lower onset potential. Particularly, the onset potential of Pt with treatment of 120 min shifts more than 100 mV negatively compared to other samples. This is consistent with the earlier Pt oxidation of 120 min sample in Fig. 3. Platinum performance toward ethanol oxidation are generally poorer than those of Pd in alkaline electrolytes [58]. The current density of 3.0 mA/cm^2, which is shown at 0.7 V of untreated Pt in Fig. 4a, is lower as compared to Pd toward ethanol oxidation in similar electrolyte (e.g. 4 mA/cm^2 in [41]). However, Pt after treatment

Table 2
Current density at 0.50 V and 0.60 V of the positive-going scan of the 1st voltammetric cycles for the electro-oxidation of 2 M ethanol 2 M KOH solution.

Period (min)	J (mA/cm^2) at 0.50 V	J (mA/cm^2) at 0.60 V
0	0.76158	1.74697
6	0.98782	2.83116
120	2.92976	6.05378
360	1.14237	2.80075

shows higher current density toward ethanol oxidation as compared to Pd. We have obtained up to 9.1 mA/cm^2 at 0.7 V for the 120 min sample a larger value as compared to that of the 360 min sample. This seems to indicate that structural modifications identified by CVs in H_2SO_4 play a major role. Indeed surface defects, steps and kinks with their low coordination numbers (CN < 8), usually exhibit very high chemical reactivity and catalytic activity for electro-oxidation of small organic molecules [59].

Things dramatically change if we look at the stability of the catalytic performance. Fig. 4b reports the current ratio between the first and the fortieth cycle for 0.5 and 0.6 V respectively. In the case of the 120 min sample the current after 40 cycles drops significantly (Fig. 4b). Particularly the recorded activity after 40 cycles is below 40% of the activity recorded in the first cycle for both 0.5 and 0.6 V. This aspect can be related to the evolution of surface structure as a result of CV cycling, and can be possibly ascribed to the lower thermodynamic stability of open shell structures [44]. The lowest degradation rate has been obtained with the 360 min sample. After 40 cycles the activity of this sample was reduced to 63% and 53% of the activity first cycle at 0.5 and 0.6 V respectively. Such results relate well with the results of the chronoamperometry experiments. 1 h stability tests at 0.5 V are reported in Fig. 5. Considerations derived from the analysis of Fig. 4b are hereby confirmed. Indeed, in terms of current density the most performing sample is the 360 min for the whole range of explored time. At the end of the experiment the current density for the 360 min sample was still 119 μA/cm^2 while the untreated samples could not deliver any appreciable current density indicating the almost completed exhaustion of the electrocatalytic activity. Pt with the longest treated period provides the best stability being the most suitable for the technological exploitation.

Ethanol electro-oxidation was also investigated by in situ FTIR spectroscopy. FTIR spectra were collected on untreated Pt and Pt after electrochemical treatment with a period of 360 min. The

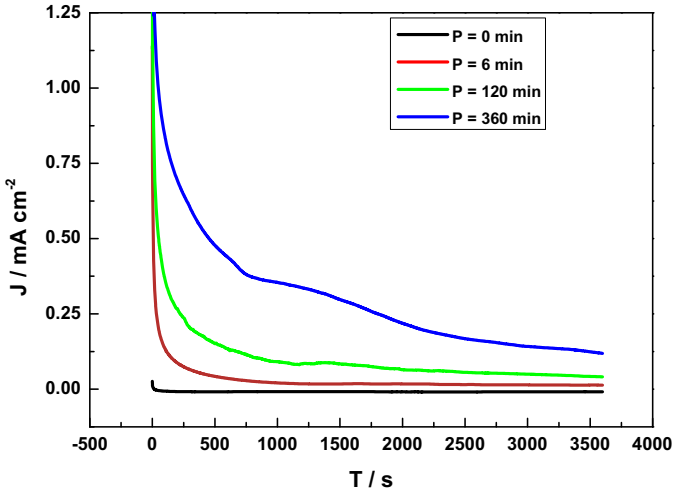

Fig. 5. Enhanced catalyst stability. Chronoamperometric curves recorded in 2 M ethanol 2 M KOH electrolytes at 0.50 V. The current is normalized by geometric area.

latter sample has been selected as it delivered the best performance in chronoamperometry. Spectra have been recorded in an electrolyte containing 2 M KOH plus 2 M ethanol solution in the 0.1–1.2 V range. For potential up to 0.2 V the only detected oxidation product, even if in tiny amount, was CO_3^{2-} (1390 cm^{-1}) for both the examined samples (Fig. 6). Formation of acetate starts at 0.3 V. It is worth noticing that the symmetric stretching vibration of COO^- (1415 cm^{-1}) cannot be resolved from the CO_3^{2-} (1390 cm^{-1}) [34]. The integrated band intensity ratio between 1415 cm^{-1} and 1550 cm^{-1} was shown in Table 3. The ratio for the treated sample is in a very steady state, around 0.84. Oppositely, the ratio for the untreated sample dropped from 1.104 to 0.889 with the potential

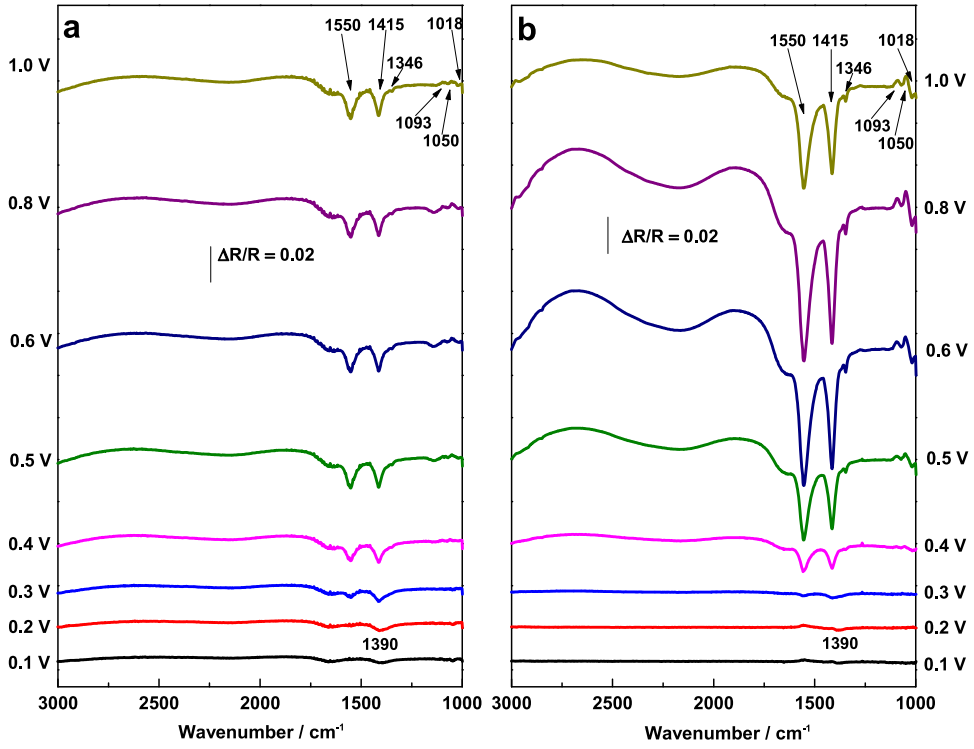

Fig. 6. Spectroelectrochemistry investigation. In situ FTIR spectra obtained under potential step polarization in 2 M ethanol 2 M KOH solution on Pt (a) before treatment; (b) after EC treatment with the treating cycle of 360 min.

Table 3
The integrated band intensity ratio between the symmetric stretching vibration of COO^- (1415 cm^{-1}) and the asymmetric stretching vibration of COO^- (1550 cm^{-1}).

Potential (V)	Band intensity ratio on Pt before treatment	Band intensity ratio on Pt after treatment with the treating cycle of 360 min
0.4	1.104	0.853
0.5	0.972	0.820
0.6	0.969	0.845
0.7	0.977	0.856
0.8	0.930	0.855
0.9	0.902	0.841
1.0	0.889	0.827

increasing from 0.4 V to 1.0 V. Particularly, all the ratios of untreated sample are larger than treated one. This indicates that in most of the explored potential range the FTIR spectra show that the formation of carbonate is negligible in the treated sample (Fig. 6b). This is not the case for the pristine polycrystalline foil for which carbonate formation occurs up to 0.5 V (Fig. 6a). Such potential values are typical of the operation conditions in fuel cells. In terms of application in a fuel cell this may not be desirable, as the C—C cleavage may require the formation of adsorbed CO leading to poisoning pathways. Ultimately this affects the stability of the device performance limiting technological exploitation. Two other downward bands at 1346 and 1018 cm^{-1} are also assigned to CH_3COO^- vibration modes. The two upward bands at 1093 and 1050 cm^{-1} are characteristic of ethanol (C—O stretching vibration), indicating its consumption as a result of the electro-oxidation. The treated sample (Fig. 6b) shows IR bands significantly more intense as compared to the untreated one (Fig. 6a). This is in good agreement with the results of chronoamperometry and CV.

4. Conclusion

We have successfully demonstrated that oxidation and subsequent reduction can be used for enhancing the electrocatalytic activity of platinum surfaces. The application of square wave potentials with high anodic (4.55 V) and high cathodic polarization (−1.95 V) enhance the active surface area up to a factor 4 as compared to pristine Pt. The frequency of the square wave has major profound implications in the evolution of the Pt surface morphology. Particularly we have found that the samples obtained with the longest period results in highest surface active surface area.

In terms of activity the most active surface has been produced with a treating period time of 120 min Nevertheless, for stability, the 360 min sample has been found to be the most performing. Structural effects may also be advocated for such an electrocatalytic activity enhancement. This might be analogous to what has been previously shown by applying similar treatments to Pd. In synthesis our findings show that the proposed electrochemical treatment could be a successful route to the reduction of the noble metal loading at the anode of alkaline direct alcohol fuel cells. Furthermore FTIR measurements have shown that treated Pt surfaces have a significantly lower tendency to provoke C—C cleavage as compared to pristine Pt. This is especially important for practical applications as without C—C cleavage no production of adsorbed CO occurs, avoiding CO poisoning. The result is important in terms of technological exploitation as it indicates that the proposed treatment allow a strategy to increase the stability of the performance of alkaline DEFCs for portable power generation.

Acknowledgments

Financial support: We gratefully acknowledge the Ente Cassa di Risparmio di Firenze for the project HYDROLAB.

We are grateful to the ICCOM CNR workshop technician Mr. Carlo Bartoli for having built the hardware for the electrochemical reforming employed in this work.

We also acknowledge Mr. Fabio Migliacci for the kind support in arranging the artwork related to the paper, Dr. Chiara Maccato and Dr. Franco Corticelli for scanning electron microscopy.

References

[1] N.M. Markovic, T.J. Schmidt, V. Stamenkovic, P.N. Ross, Fuel Cells 1 (2001) 105–116.
[2] K.J.J. Mayrhofer, M. Arenz, B.B. Blizanac, V. Stamenkovic, P.N. Ross, N.M. Markovic, Electrochim. Acta 50 (2005) 5144–5154.
[3] E. Yoo, T. Okata, T. Akita, M. Kohyama, J. Nakamura, I. Honma, Nano Lett. 9 (2009) 2255–2259.
[4] Y.J. Li, Y.J. Li, E.B. Zhu, T. McLouth, C.Y. Chiu, X.Q. Huang, Y. Huang, J. Am. Chem. Soc. 134 (2012) 12326–12329.
[5] A. Brouzgou, S.Q. Song, P. Tsiakaras, Appl. Catal. B: Environ. 127 (2012) 371–388.
[6] N. Tian, Z.Y. Zhou, S.G. Sun, Y. Ding, Z.L. Wang, Science 316 (2007) 732–735.
[7] W.J. Zhou, Z.H. Zhou, S.Q. Song, W.Z. Li, G.Q. Sun, P. Tsiakaras, Q. Xin, Appl. Catal. B: Environ. 46 (2003) 273–285.
[8] A.V. Tripkovic, K.D. Popovic, B.N. Grgur, B. Blizanac, P.N. Ross, N.M. Markovic, Electrochim. Acta 47 (2002) 3707–3714.
[9] S. Rousseau, C. Coutanceau, C. Lamy, J.M. Leger, J. Power Sources 158 (2006) 18–24.
[10] H.S. Liu, C.J. Song, L. Zhang, J.J. Zhang, H.J. Wang, D.P. Wilkinson, J. Power Sources 155 (2006) 95–110.
[11] S. Wasmus, A. Kuver, J. Electroanal. Chem. 461 (1999) 14–31.
[12] V. Bambagioni, C. Bianchini, Y.X. Chen, J. Filippi, P. Fornasiero, M. Innocenti, A. Lavacchi, A. Marchionni, W. Oberhauser, F. Vizza, ChemSusChem 5 (2012) 1266–1273.
[13] V. Bambagioni, C. Bianchini, J. Filippi, W. OberhauserIal, A. Marchionni, F. Vizza, R. Psaro, L. Sordelli, M.L. Foresti, M. Innocenti, ChemSusChem 2 (2009) 99–112.
[14] E. Antolini, J. Power Sources 170 (2007) 1–12.
[15] E.S. Steigerwalt, G.A. Deluga, D.E. Cliffel, C.M. Lukehart, J. Phys. Chem. B 105 (2001) 8097–8101.
[16] W.J. Zhou, S.Q. Song, W.Z. Li, Z.H. Zhou, G.Q. Sun, Q. Xin, S. Douvartzides, P. Tsiakaras, J. Power Sources 140 (2005) 50–58.
[17] F. Colmati, E. Antolini, E.R. Gonzalez, J. Power Sources 157 (2006) 98–103.
[18] H.Q. Li, G.Q. Sun, L. Cao, L.H. Jiang, Q. Xin, Electrochim. Acta 52 (2007) 6622–6629.
[19] L.H. Jiang, G.Q. Sun, S.G. Sun, J.G. Liu, S.H. Tang, H.Q. Li, B. Zhou, Q. Xin, Electrochim. Acta 50 (2005) 5384–5389.
[20] K. Han, J. Lee, H. Kim, Electrochim. Acta 52 (2006) 1697–1702.
[21] J.J. Baschuk, X.G. Li, Int. J. Energy Res. 25 (2001) 695–713.
[22] Q.F. Li, R.H. He, J.A. Gao, J.O. Jensen, N.J. Bjerrum, J. Electrochem. Soc. 150 (2003) A1599–A1605.
[23] U. Bardi, C. Borri, A. Lavacchi, A. Tolstogouzov, E.B. Trunin, O.E. Trunina, Scr. Mater 60 (2009) 423–426.
[24] T.E. Graedel, Annu. Rev. Mater. Res. 41 (2011) 323–335.
[25] J.S. Spendelow, D.C. Papageorgopoulos, Fuel Cells 11 (2011) 775–786.
[26] D.F. van der Vliet, C. Wang, D. Tripkovic, D. Strmcnik, X.F. Zhang, M.K. Debe, R.T. Atanasoski, N.M. Markovic, V.R. Stamenkovic, Nat. Mater 11 (2012) 1051–1058.
[27] H.A. Gasteiger, N. Markovic, P.N. Ross, E.J. Cairns, J. Phys. Chem. U. S. 98 (1994) 617–625.
[28] H.A. Gasteiger, N.M. Markovic, P.N. Ross, J. Phys. Chem. U. S. 99 (1995) 16757–16767.
[29] N.M. Markovic, H.A. Gasteiger, P.N. Ross, X.D. Jiang, I. Villegas, M.J. Weaver, Electrochim. Acta 40 (1995) 91–98.
[30] T. Yajima, H. Uchida, M. Watanabe, J. Phys. Chem. B 108 (2004) 2654–2659.
[31] M.T.M. Koper, T.E. Shubina, R.A. van Santen, J. Phys. Chem. B 106 (2002) 686–692.
[32] Y.Y. Tong, H.S. Kim, P.K. Babu, P. Waszczuk, A. Wieckowski, E. Oldfield, J. Am. Chem. Soc. 124 (2002) 468–473.
[33] S.R. Brankovic, J.X. Wang, R.R. Adzic, Electrochem. Solid State Lett. 4 (2001) A217–A220.
[34] Z.Y. Zhou, Q.A. Wang, J.L. Lin, N. Tian, S.G. Sun, Electrochim. Acta 55 (2010) 7995–7999.
[35] J. Mann, N. Yao, A.B. Bocarsly, Langmuir 22 (2006) 10432–10436.
[36] S.C.S. Lai, M.T.M. Koper, Faraday Discuss. 140 (2008) 399–416.
[37] D.J. Tarnowski, C. Korzeniewski, J. Phys. Chem. B 101 (1997) 253–258.
[38] F. Colmati, G. Tremiliosi-Filho, E.R. Gonzalez, A. Berná, E. Herrero, J.M. Feliu, Faraday Discuss. 140 (2008) 379–397.
[39] A. Kowal, M. Li, M. Shao, K. Sasaki, M.B. Vukmirovic, J. Zhang, N.S. Marinkovic, P. Liu, A.I. Frenkel, R.R. Adzic, Nat. Mater. 8 (2009) 325–330.
[40] Y.X. Chen, A. Lavacchi, S.P. Chen, F. di Benedetto, M. Bevilacqua, C. Bianchini, P. Fornasiero, M. Innocenti, M. Marelli, W. Oberhauser, S.G. Sun, F. Vizza, Angew. Chem. Int. Edit. 51 (2012) 8500–8504.
[41] L.Q. Wang, M. Bevilacqua, Y.X. Chen, J. Filippi, M. Innocenti, A. Lavacchi, A. Marchionni, H. Miller, F. Vizza, J. Power Sources 242 (2013) 872–876.
[42] D. Chen, Q. Tao, L.W. Liao, S.X. Liu, Y.X. Chen, S. Ye, Electrocatalysis 2 (2011) 207–219.
[43] K. Ashley, S. Pons, Chem. Rev. 88 (1988) 673–695.

[44] B.E. Conway, Progr. Surf. Sci. 49 (1995) 331–452.
[45] X.P. Wang, R. Kumar, D.J. Myers, Electrochem. Solid State Lett. 9 (2006) A225–A227.
[46] N. Furuya, S. Koide, Surf. Sci. 220 (1989) 18–28.
[47] N.M. Markovic, B.N. Grgur, P.N. Ross, J. Phys. Chem. B 101 (1997) 5405–5413.
[48] C. Coutanceau, P. Urchaga, S. Brimaud, S. Baranton, Electrocatalysis 3 (2012) 75–87.
[49] J. Solla-Gullon, F.J. Vidal-Iglesias, E. Herrero, J.M. Feliu, A. Aldaz, Electrochem. Commun. 8 (2006) 189–194.
[50] J. Clavilier, D. Armand, S.G. Sun, M. Petit, J. Electroanal. Chem. 205 (1986) 267–277.
[51] W.E. Triaca, A.J. Arvia, J. Appl. Electrochem. 20 (1990) 347–356.
[52] H. Yang, W. Vogel, C. Lamy, N. Alonso-Vante, J. Phys. Chem. B 108 (2004) 11024–11034.
[53] N. Tian, Z.Y. Zhou, S.G. Sun, J. Phys. Chem. C 112 (2008) 19801–19817.
[54] Z.X. Liang, T.S. Zhao, J.B. Xu, L.D. Zhu, Electrochim. Acta 54 (2009) 2203–2208.
[55] X. Fang, L.Q. Wang, P.K. Shen, G.F. Cui, C. Bianchini, J. Power Sources 195 (2010) 1375–1378.
[56] C. Bianchini, P.K. Shen, Chem. Rev. 109 (2009) 4183–4206.
[57] S.C.S. Lai, M.T.M. Koper, Phys. Chem. Chem. Phys. 11 (2009) 10446–10456.
[58] C.W. Xu, P.K. Shen, Y.L. Liu, J. Power Sources 164 (2007) 527–531.
[59] Z.Y. Zhou, Z.Z. Huang, D.J. Chen, Q. Wang, N. Tian, S.G. Sun, Angew. Chem. Int. Edit. 49 (2010) 411–414.